EPSC Abstracts
Vol. 13, EPSC-DPS2019-832-2, 2019
EPSC-DPS Joint Meeting 2019

EPSC
EPSC-DPS Joint Meeting 2019
15–20 September 2019 | Geneva, Switzerland

The Europa Imaging System (EIS): High-Resolution, 3-D Insight into Europa's Geology, Ice Shell, and Potential for Current Activity

E. P. Turtle (1), A. S. McEwen (2), M. Bland (3), G. C. Collins (4), I. J. Daubar (5), C. M. Ernst (1), L. Fletcher (6), C. J. Hansen (7), S. E. Hawkins (1), A. G. Hayes (8), D. Humm (1), T. A. Hurford (9), R. L. Kirk (3), N. Kutsop (8), A. C. Barr Mlinar (7), F. Nimmo (10), G. W. Patterson (1), C. B. Phillips (5), A. Pommerol (11), L. Prockter (12), L. C. Quick (13), E. L. Reynolds (1), K. A. Slack (1), J. M. Soderblom (14), S. Sutton (2), N. Thomas (11), H. Winters (1)
(1) Johns Hopkins Applied Physics Laboratory, Laurel, Maryland, USA, (2) Univ. Arizona, Tucson, Arizona, USA, (3) U.S. Geological Survey, Flagstaff, AZ, USA, (4) Wheaton College, Norton, MA, USA, (5) Jet Propulsion Laboratory, Pasadena, CA, USA, (6) Univ. Leicester, Leicester, UK, USA, (7) Planetary Science Institute, Tucson, AZ, USA, (8) Cornell Univ., Ithaca, NY, USA, (9) NASA Goddard Space Flight Center, Greenbelt, MD, USA, (10) Univ. California, Santa Cruz, CA, USA, (11) Univ. Bern, Bern, Switzerland, USA, (12) Lunar and Planetary Institute, Houston, TX, USA, (13) Smithsonian Institution, Washington, DC, USA, (14) Massachusetts Institute of Technology, Cambridge, MA, USA.
(Elizabeth.Turtle@jhuapl.edu)

Abstract

Designed for NASA's *Europa Clipper* Mission [1–3], EIS combines a narrow-angle camera and a wide-angle camera (Fig. 1), each with framing and pushbroom imaging capability, to explore Europa and address high-priority geology, composition, ice shell and ocean science objectives. EIS data will be used to generate: cartographic and geologic maps; regional and high-resolution topography; GIS, color, and photometric data products; a database of plume-search observations; and control points tied to radar altimetry [4]. These datasets will allow us to:

- constrain formation processes of landforms by characterizing geologic structures, units, and global cross-cutting relationships [5];
- identify relationships to subsurface structures and potential near-surface water [e.g., 6] detected by ice-penetrating radar [7];
- investigate compositional variability between and among landforms and correlate composition between individual features and regional units;
- search for evidence of recent or current activity, including potential erupting plumes [e.g., 8–11];
- constrain ice-shell thickness;
- characterize surface clutter to aid interpretation of deep and shallow radar sounding [7];
- characterize scientifically compelling landing sites and hazards by determining the nature of the surface at meter scales [12–14].

1. EIS Narrow-angle Camera (NAC)

The NAC, with a 2.3° x 1.2° field of view (FOV) and a 10-µrad instantaneous FOV (IFOV), achieves 0.5-m pixel scale over a 2-km-wide swath from 50-km altitude. A 2-axis gimbal enables independent targeting, allowing near-global (>90%) mapping of Europa at ⩽100-m pixel scale (to date, only ~14% of Europa has been imaged at ⩽500 m/pixel), as well as regional stereo imaging. The gimbal slew rate is designed to be able to perform very high-resolution stereo imaging from as close as 50-km altitude during high-speed (~4.5 m/s) flybys to generate digital topographic models (DTMs) with 2-m spatial scale and 0.25-m vertical precision. The NAC will also perform high-phase-angle observations to search for potential erupting plumes [8–11]; a pixel scale of 10 km from 10^6 km range means that the NAC can take advantage of good illumination geometry for forward scattering by potential plumes even when the spacecraft is distant from Europa.

2. EIS Wide-angle Camera (WAC)

The WAC has a 48° x 24° FOV, with a 218-µrad IFOV, and is designed to acquire 3-line pushbroom stereo swaths along flyby ground-tracks. From an altitude of 50 km, the WAC achieves 11-m pixel scale over a 44-km-wide swath, generating DTMs with 32-m spatial scale and 4-m vertical precision. These data also support characterization of surface clutter for interpretation of radar deep and shallow sounding modes.

3. Detectors and Electronics

The cameras have identical rapid-readout, radiation-hard 4k x 2k CMOS detectors [15] and can image in both pushbroom and framing modes. Color observations are acquired by pushbroom imaging using six broadband filters (~350–1050 nm; Table 1), allowing mapping of surface units for correlation with geologic structures, topography, and compositional units from other instruments [e.g., 16]. APL's radiation-hardened data processing units (DPU) take full advantage of the rapid, random-access readout of the CMOS arrays and use real-time processing for pushbroom imaging [17], including: WAC 3-line stereo, digital time delay integration (TDI) to enhance signal-to-noise ratios (SNR), and readout strategies to measure and correct pointing jitter [18].

4. Summary

EIS will achieve unprecedented near-global imaging coverage of the surface of Europa at better than 100-m pixel scale, as well as local high-resolution imaging (≤1-m pixel scale), color imaging, and topographic models. EIS data sets and collaborative science with other *Europa Clipper* investigations will provide insight into Europa's global geology, ice shell, and the potential for recent or current activity, to fulfill the goal of exploring Europa to investigate its habitability.

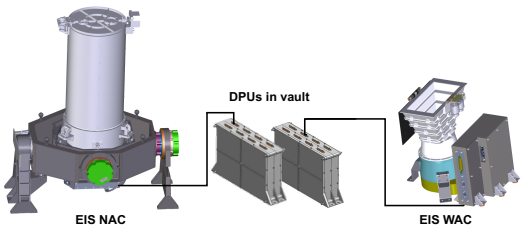

Figure 1: (Left) EIS NAC, mounted on 2-axis gimbal. (Middle) EIS DPUs. (Right) EIS WAC.

Acknowledgements

This work is supported by NASA's *Europa Clipper* Mission.

Table 1: NAC and WAC have six broad-band, stripe filters for color pushbroom imaging to map surface units for correlation with geologic structures, and compositional units identified by other instruments.

Filter	Key Uses	Wavelength (nm)
Clear	Surface mapping, stereo, context imaging, best SNR for faint targets, e.g., plume searches	NAC: 350–1050 WAC: 370–1050
NUV	Surface color; plumes w/ Rayleigh scattering	NAC: 355–400 WAC: 375–400
BLU	Surface color; Rayleigh scattering w/ NUV	380–475
GRN	Surface color; airglow	520–590
RED	Surface color	640–700
IR1	Surface color; continuum for H_2O band	780–920
1μm	Surface color; coarse-grained ice H_2O band	950–1050

References

[1] Korth H. et al., *COSPAR,* #B5.3-0032-18, 2018.

[2] Pappalardo R.T. et al., *AGU Fall Mtg.*, #P53H-08, 2017.

[3] Pappalardo R.T. et al., *EPSC*, #EPSC2017-304, 2017.

[4] Steinbrügge G. et al., *EPSL 482*, pp. 334-341, 2018.

[5] Collins G.C. et al., *LPSC 49*, #2625, 2018.

[6] Schmidt B.E. et al., *Nature 479*, 502-505, 2015.

[7] Moussessian A. et al., *AGU Fall Mtg.*, #P13E-05, 2015.

[8] Jia X. et al., *Nature Astronomy 2*, pp. 459–464, 2018.

[9] Sparks W.B. et al., *Ap. J. 839*:L18, 2017.

[10] Roth L. et al., *Science 343*, 171-174, 2014.

[11] Quick L. et al., *Planet. Space Sci. 86*, 1-9, 2013.

[12] Hand K.P. et al., *COSPAR*, #B5.3-0033-18, 2018.

[13] Hand K.P. et al., LPSC 49, #2600, 2017.

[14] Pappalardo R.T. et al., *Astrobiol. 13*, 740-773, 2013.

[15] Janesick J. et al., *Proc. SPIE 9211*, 921106, 2014.

[16] Blaney D.L. et al., *LPSC 50, #2218, 2019.*

[17] McEwen A.S. et al., *Intl. Wkshp. Instr. Planet. 1*, 1041, 2012.

[18] Sutton S.S. et al., *ISPRS, XLII-3/W1*, pp. 141-148, 2017.